Vector-Valued Intensity Measures to Predict Peak and Hysteretic Energy Demands of 3D R/C Buildings

José I. Torres, Edén Bojórquez, Alfredo Reyes, and Juan Bojórquez

Abstract In this study, several peak and energy vector-valued ground motion intensity measures (*IMs*) are proposed to predict maximum inter-story drift and hysteretic energy demands of 3D reinforced concrete (R/C) buildings subjected to narrow-band motions. The selected vector-valued *IMs* are based on the spectral acceleration, pseudo-velocity, velocity and input energy at first mode of the structure as first component. As the second component, ground motion parameters based on peak, integral and spectral shape proxies such as the well-known N_p are used. The objective of the present study is to provide vector-valued *IMs* whit the ability to predict the maximum inter-story drift and hysteretic energy demands on 3D framed structures. It is observed that vector-valued *IMs* based on N_p provide a high relation whit maximum inter-story drift and hysteretic energy demands of reinforced concrete framed buildings.

Keywords 3D buildings · Hysteretic energy · Intensity measure · Reinforced concrete · Structural dynamics · Vector-valued

1 Introduction

Since the beginning of earthquake engineering and seismology, several studies have been developed to provide a parameter with the ability to characterize the ground motion potential of an earthquake which is known as ground motion intensity

J. I. Torres (✉) · E. Bojórquez · A. Reyes · J. Bojórquez
Facultad de Ingeniería, Universidad Autónoma de Sinaloa, Culiacán 80040, México

E. Bojórquez
e-mail: eden@uas.edu.com.mx

A. Reyes
e-mail: reyes@uas.edu.mx

J. Bojórquez
e-mail: juanbmu@uas.edu.mx

A. Benavent-Climent and F. Mollaioli (eds.), *Energy-Based Seismic Engineering*,
Lecture Notes in Civil Engineering 155,
https://doi.org/10.1007/978-3-030-73932-4_18

measure. The most important characteristic of an *IM* is the reduction of the uncertainty in the estimation of the seismic response of structures under earthquakes (efficiency). In others words, the efficiency is defined as the ability to predict the response of structures subjected to earthquakes with low uncertainty. Although, several studies have been developed to propose or to analyze ground motion intensity measures [1–18]. In most of the cases, the proposed *IMs* are based in the prediction of maximum demands such as maximum ductility and inter-story drift. By other hand, nowadays, several studies promote the use of vector-valued or scalar ground motion *IMs* based on spectral shape, because they predict with good accuracy the maximum inter-story drift and maximum ductility of structures subjected to earthquakes [12–15, 17–20]. In particular, vector and scalar ground motion intensity measures based on N_p which are representative of the spectral shape have resulted very well correlated with the nonlinear structural response [18, 20, 21]. However, as it was mentioned before, an appropriated *IMs* should be capable of predicting all types of engineering demand parameters, as example, hysteretic energy demands. Hysteretic energy demands are very important in structures when subjected to long duration narrow-band ground motions [22–28]. In this study, vector-valued ground motion intensity measures have been proposed in order to predict the seismic response of 3D reinforced concrete buildings under narrow-band motions recorded at the soft soil site of Mexico City. The proposed *IMs* are separated in 2 sets, the first one is composed by vector-valued *IMs* with maximum peak ground and integral response, and the second set by vector-valued *IMs* with spectral shape parameters as is the case of the N_p parameter. For the evaluation of the vector-valued *IMs*, the maximum inter-story drift and the hysteretic energy demand are used as engineering demand parameters. It is important to say that hysteretic energy demand is not commonly used in efficiency studies of *IMs* in comparison with the maximum inter-story drift or peak demands. So far, this study differs from others by the use of 3D structures, as well as the use of both performance parameters (maximum inter-story drift and the hysteretic energy demand). Finally, an optimization of the N_p parameter for the selected spectral shape vector-valued *IMs* developed through the values of $Sa(T_1)$, $Sv(T_1)$, $V(T_1)$ and $E_I(T_1)$ is computing in the present study.

2 Methodology

2.1 Vector-Valued Ground Motion Intensity Measures

The prediction of the seismic response is estimated considering 32 different vector-valued ground motion *IMs*, which are divided in 2 sets of 16 *IMs*. The first set is based on traditional peak and integral *IMs*, while the second is based on the proxy of the spectral shape named N_p. For both sets the parameters $Sa(T_1)$, $Sv(T_1)$, $V(T_1)$ and $E_I(T_1)$ are considered: where, *Sa* is the spectral acceleration, *Sv* is the pseudo-velocity, *V* is the velocity, E_I is the input energy and T_1 is the first mode of vibration.

Note that E_I can be defined from the equation of motion of a single degree of freedom system as follows:

$$m\ddot{x}(t) + c\dot{x} + f_s(x, \dot{x}) = -m\ddot{x}_g(t) \tag{1}$$

In Eq. (1), m is the mass of the system; c, the viscous damping coefficient; $f_s(x, \dot{x})$, the non-linear force; $\ddot{x}$, the ground acceleration; and x, the displacement with respect to the base of the system. A dot above x indicates a derivative with respect to time. In case of an elastic linear systems, $f_s(x, \dot{x}) = kx$, where k is the stiffness of the system.

Integrating each member of Eq. (1) with respects to x, yields:

$$\int m\ddot{x}(t)dx + \int c\dot{x}(t)dx + \int f_s(x, \dot{x})dx = -\int m\ddot{x}_g(t)dx \tag{2}$$

Equation (2) can be written as energy balanced equation as follows [29]:

$$E_K + E_D + E_S + E_H = E_I \tag{3}$$

where E_K, E_D, E_S and E_H represent the kinetic (K), viscous damping (D), deformation (S) and dissipated hysteretic (H) energies, respectively; and E_I is the relative input energy.

For the set number 1, the parameters *PGA*, *PGV*, t_D and I_D are used as second component of the vector-valued *IMs*; where *PGA* represents peak ground acceleration, *PGV* peak ground velocity, and finally, t_D and I_D, represents the effective duration of the earthquake [30] and the accumulated potential [4], respectively. The effective duration (t_D) is defined as the time interval between 5% and 95% of the Arias Intensity [2], which is obtained from the following equation:

$$I_A = \int_0^T a^2(t)dt \tag{4}$$

where T is the total duration of the earthquake. In addition, the I_D factor is defined as:

$$I_D = \frac{\int_0^T a(t)^2 dt}{PGA \cdot PGV} \tag{5}$$

Table 1 shows a summary of the selected vector-valued *IMs* of the first set. The first column indicates the ground motion *IMs*; the second, third and fourth columns, indicate if the *IMs* are based on peak ground response, duration and/or spectral shape response, respectively.

In the second set of vector-valued *IMs*, the parameter N_p is used as the second component of the vector-valued *IMs* to determine the spectral shape [18]. The general form of the N_p generalized parameter is defined in the following equation:

Table 1 First set of vector-valued *IMs*

Intensity measures	Peak ground response	Duration	Spectral shape
$<Sa(T_1), PGA>$	*		
$<Sa(T_1), PGV>$	*		
$<Sa(T_1), t_D>$	*	*	
$<Sa(T_1), I_D>$	*	*	
$<Sv(T_1), PGA>$	*		
$<Sv(T_1), PGV>$	*		
$<Sv(T_1), t_D>$	*	*	
$<Sv(T_1), I_D>$	*	*	
$<V(T_1), PGA>$	*		
$<V(T_1), PGV>$	*		
$<V(T_1), t_D>$	*	*	
$<V(T_1), I_D>$	*	*	
$<E_I(T_1), PGA>$	*	*	
$<E_I(T_1), PGV>$	*	*	
$<E_I(T_1), t_D>$	*	*	
$<E_I(T_1), I_D>$	*	*	

$$N_{pg} = \frac{S_{avg}(T_i, \ldots, T_f)}{S(T_j)} \tag{6}$$

From the Eq. (6), $S(T_j)$ represents a spectral parameter taken from any type of spectrum as in the case of acceleration, velocity, displacement, input energy, inelastic parameters and so on, at period T_j. $S_{avg}(T_i, \ldots, T_f)$ is the geometrical mean of a specific spectral parameter between the range of periods T_i and T_f. Note that the periods T_i and T_j could be different. N_{pg} is similar to the traditional definition of N_p [10] but for different types of spectra and a wider range of periods. In such a way that

parameters as the traditional N_p or the recently proposed Sa_{Ratio} [31] are particular cases of the generalized spectral shape parameter N_{pg}. If the pseudo-acceleration spectrum is used, and $T_i = T_j = T_1$ (first mode structural vibration period) N_{pg} is equal to the traditional N_p. If the value of N_p is lower than one, we can expect that the average spectrum with negative slope in the range of periods between T_i and T_f, if N_p is equal to one, the average spectrum is to about flat in the same range of periods, and in the case of N_p is larger than one, we can expect an increasing trend of the spectra beyond T_i. In this work, 10 points are used to calculate the average spectrum, a value of $S(T_j)$ equal to T_1, and the values of T_i and T_f, were obtained through an optimization study as will be observed below. In Table 2 a summary of the selected vector-valued *IMs* for the second set is illustrated.

2.2 Structural 3D Reinforced Concrete Frames Models

Two 3D R/C frames having 7 and 10 stories were considered for the studies reported herein. The 3D frames are denoted as F7 and F10 respectively (see Fig. 1). The frames, designed according to the Mexico City Seismic Design Provisions (MCSDP). It was considered that the elements (beams and columns) of the structures have a hysteretic behavior similar to the modified Takeda model to represent the non-linearity of the material. The main characteristics of the 3D R/C models are shown in Table 3. Note that column eight in Table 3 represents the fundamental period of vibration of the structure.

2.3 Earthquake Ground Motion Records

To determine the seismic performance of the two 3D R/C frames, a dynamic analysis is carried out. For this aim, the structures are subjected under the action of seismic records representative of the site in which they are assumed to be displaced. In this work it is assumed that the buildings are located at soft soil of Mexico City and are subject to narrow band seismic ground motions. The following table indicates the narrow band accelerograms obtained from the soft soil of Mexico City used in the present study (Table 4).

2.4 Scaling of Seismic Records

The seismic records or accelerograms were scaled to represent seismic events of different intensities, and thus to determine the responses of the modeled structures in terms of the maximum inter-story drifts and the hysteretic energy demands, which allows to compare the efficiency of the different *IMs* used in this work. For the

Table 2 Second set of vector-valued *IMs*

Intensity measures	Peak ground response	Duration	Spectral shape
$<Sa(T_1), N_{pSa}>$	*		*
$<Sa(T_1), N_{pSv}>$	*		*
$<Sa(T_1), N_{pV}>$	*		*
$<Sa(T_1), N_{pEI}>$	*	*	*
$<Sv(T_1), N_{pSa}>$	*		*
$<Sv(T_1), N_{pSv}>$	*		*
$<Sv(T_1), N_{pV}>$	*		*
$<Sv(T_1), N_{pEI}>$	*	*	*
$<V(T_1), N_{pSa}>$	*		*
$<V(T_1), N_{pSv}>$	*		*
$<V(T_1), N_{pV}>$	*		*
$<V(T_1), N_{pEI}>$	*	*	*
$<E_I(T_1), N_{pSa}>$	*	*	*
$<E_I(T_1), N_{pSv}>$	*	*	*
$<E_I(T_1), N_{pV}>$	*	*	*
$<E_I(T_1), N_{pEI}>$	*	*	*

scaling of the seismic records the combination of the horizontal components of the earthquake was used [see Eq. (7)]. The scaling was done to have specific values in the response spectra in a given period (the period of interest, which is the fundamental period of the structures was used). The parameters to scale the records are $Sa(T_1)$, $Sv(T_1)$, $V(T_1)$ and $E_I(T_1)$.

$$IMs = \sqrt{\left(IMs_{Comp1}\right)^2 + \left(IMs_{Comp2}\right)^2} \tag{7}$$

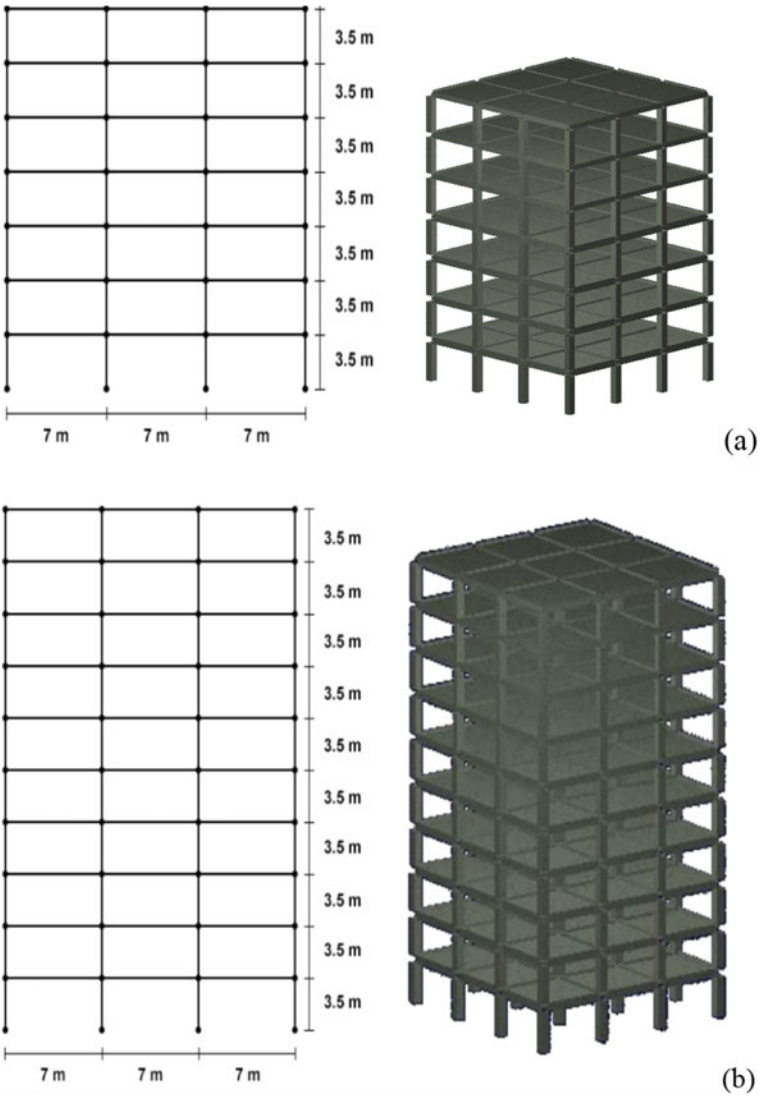

Fig. 1 F4 (**a**) and F10 (**b**) frame models

Table 3 Characteristics of the 3D R/C models

Frame	Number of stories	T_1(s)
F7	7	0.7
F10	10	0.98

Table 4 Selected narrow-band ground motion records

No	Date	Magnitude	Station
1	97-01-11	6.9	VALLE GÓMEZ
2	95-10-09	7.3	VALLE GÓMEZ
3	89-04-25	6.9	TLATELOLCO
4	95-09-14	7.4	TLATELOLCO
5	97-01-11	6.9	TLATELOLCO
6	89-04-25	6.9	GARIBALDI
7	95-09-14	7.2	GARIBALDI
8	95-10-09	7.3	GARIBALDI
9	97-01-11	6.9	GARIBALDI
10	95-09-14	7.2	ALAMEDA
11	89-04-25	6.9	ALAMEDA
12	89-04-25	6.9	TLATELOLCO
13	95-09-14	7.2	TLATELOLCO
14	95-10-09	7.3	LIVERPOOL
15	97-01-11	6.9	LIVERPOOL
16	95-09-14	7.2	CORDOBA
17	95-10-09	7.3	CORDOBA
18	97-01-11	6.9	CORDOBA
19	89-04-25	6.9	C.U. JUAREZ
20	95-09-14	7.2	C.U. JUAREZ
21	95-10-09	7.3	C.U. JUAREZ
22	97-01-11	6.9	C.U. JUAREZ
23	95-09-14	7.2	CUJP
24	95-10-09	7.3	CUJP
25	97-01-11	6.9	CUJP
26	85-09-19	8.1	SCT B-1
27	89-04-25	6.9	SCT B-2
28	89-04-25	6.9	SECTOR POPULAR
29	95-09-14	7.2	SECTOR POPULAR
30	95-10-09	7.3	SECTOR POPULAR
31	97-01-11	6.9	SECTOR POPULAR

In Eq. (7), while *IMs* is the selected intensity measure that represent the combination of both directions of the ground motion (i.e. *Sa*, *Sv*, *V* and E_I), IMs_{Comp1} and IMs_{Comp2} are the intensity measure in each horizontal component orthogonal.

2.5 *Performance Parameters*

The engineering demand parameters selected were the maximum inter-story drift and the normalized hysteretic energy by the mass (E_N), Eq. (8). These parameters are selected due to their importance for seismic design purposes, since they capture both information about maximum demands and the effect on the duration of the earthquake and with the cumulative demands [32]. In fact, currently various damage indexes have been proposed based on hysteretic energy [33–35].

$$E_N = \frac{E_H}{m} \tag{8}$$

3 Numerical Results

3.1 *Relation Between Vector-Valued* IMs *and the Structural Demand of 3D R/C Fames*

Baker and Cornell [14] and Bojórquez and Iervolino [18] showed the advantages of using vector-valued ground motion intensity measures instead of scalars. The main advantage is the increasing in the efficiency to predict the structural response. Herein with the aim to obtain the relation between the structural response of R/C frames and the vectors selected; nonlinear incremental dynamic analysis was used to obtain the seismic response of the R/C frames subjected to the 31 ground motion records by using the first parameter of the vector and then the relation between the structural response of the R/C frames and the second parameter of the vector is obtained. Figure 2a shows a general illustrative example of the incremental dynamic

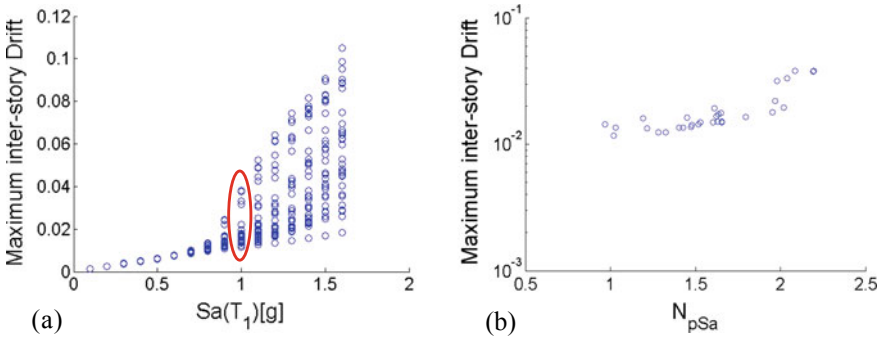

Fig. 2 **a** Illustrative example of incremental dynamic analysis scaling for $Sa(T_1)$; **b** relation between N_{pSa} and Maximum inter-story drift at $Sa(T_1) = 1$g

analysis for Sa(T_1) in terms of the maximum inter-story drift. It is observed a poor relation among Sa(T_1) and maximum inter-story drift, in fact the uncertainty to predict maximum inter-story drift using the spectral acceleration tend to increase with the intensity of the earthquake ground motion. Figure 2b illustrates the relation obtained for $<Sa(T_1), N_{pSa}>$ and the maximum inter-story drift when $Sa(T_1) = 1$ g (see the values in the circle of Fig. 2b). Note the good relation between N_{pSa} and the maximum inter-story drift reflecting the advantage of using the vector-valued ground motion intensity measure. It explains the reduction in the uncertainty associated with the structural response when vector-valued parameters are selected as intensity measures, and this type of intensity measures could be more efficient for nonlinear structural response prediction.

3.2 *Optimization of the* $\mathbf{N_p}$ *Parameter*

As it was mentioned above, a study was carried out to determine the value of T_i and T_f to be used for the N_p spectral shape parameter of the second set of intensity measures. For this reason, pairs of T_i values were created ranging from 0.1 * T_1 to 1.0 * T_1, and T_f from 1.1 * T_1 to 3.0 * T_1. The value of N_p of all the pairs was calculated, applied to the 16 vector-valued spectral shape *IMs* and were selected the values for which T_i and T_f minimize the standard deviation of the natural logarithm of the seismic response (maximum inter-story drift or hysteretic energy) of the R/C buildings.

A summary of the optimal T_i and T_f values computed for the F7 R/C frame is presented in Table 5 and for the F10 R/C frame in Table 6. It is observed in general, that the value of the initial period T_i is equal to T_1, while for T_f, a value between 2.0 and 3.0 times T_1 is suggested, which is valid for the two selected performance parameters (maximum inter-story drift and normalized hysteretic energy).

3.3 *Efficiency of Selected Vector-Valued Ground Motion* IMs

The numerical results of this work are described here. To show the effectiveness of the selected vector-valued *IMs*, the standard deviation values of the natural logarithm of the maximum inter-story drift and the hysteretic energy demands, obtained from the incremental dynamic analysis at different levels of intensities are presented. Standard deviations were estimated using a linear regression for all cases and scaling levels of *IMs* used, and of the R/C framed building considered. Figure 3 shows the results obtained for the vector-valued *IMs* that use as first component $Sa(T_1)$, in terms of the maximum inter-story drift for both frames; and, Fig. 4 shows the same results, but now, in terms of the hysteretic energy demands. By other hand, Fig. 5 shows the results obtained for vector-valued *IMs* that use EI as first component, in terms of the maximum inter-story drift, for the two 3D R/C frames; and, Fig. 6, shows

Table 5 Optimal T_i and T_f values for the 16 vector-valued spectral shape *IMs* to predict the seismic response of F7 R/C frame

IMs	Inter-story drift		Normalized hysteretic energy	
	T_i/T_1	T_f/T_1	T_i/T_1	T_f/T_1
$<Sa(T_1), N_{pSa}>$	1	3	1	3
$<Sa(T_1), N_{pSv}>$	1	3	1	3
$<Sa(T_1), N_{pV}>$	1	3	1	3
$<Sa(T_1), N_{pEI}>$	1	3	1	3
$<Sv(T_1), N_{pSa}>$	1	3	1	3
$<Sv(T_1), N_{pSv}>$	1	3	1	3
$<Sv(T_1), N_{pV}>$	1	3	1	3
$<Sv(T_1), N_{pEI}>$	1	3	1	3
$<V(T_1), N_{pSa}>$	1	3	1	3
$<V(T_1), N_{pSv}>$	1	3	1	3
$<V(T_1), N_{pV}>$	1	3	1	3
$<V(T_1), N_{pEI}>$	1	3	1	3
$<E_I(T_1), N_{pSa}>$	0.3	1.1	1	3
$<E_I(T_1), N_{pSv}>$	0.3	1.1	0.3	1.1
$<E_I(T_1), N_{pV}>$	1	3	1	3
$<E_I(T_1), N_{pEI}>$	0.3	1.1	1	3

the same results, but, in terms of the hysteretic energy demands. Note that since the results generated by vector-valued *IMs* that use $Sv(T_1)$ and $V(T_1)$ as first component have low efficiency than $Sa(T_1)$, only the results of the *IMs* that use $Sa(T_1)$ as the first component have been included for the sake of brevity. In addition, with the aim to have a comparison in terms of input energy, also this parameter was plotted when represent the first component of the vector. It can be seen that the vector-valued *IMs* that use spectral shape parameters N_p are more efficient to predict the seismic demands (peak and cumulative) for every frame, especially those based on spectral acceleration or velocity (N_{pSa}, N_{pSv}, N_{pV}). By the other hand, the peak ground response and duration parameters of the first set of *IMs* are not good estimators of the maximum inter-story drift and the normalized hysteretic energy demands, because they produce large uncertainties. Finally, it is observable that the selected vector-valued *IMs* are more efficient in predicting the maximum inter-story drift than the hysteretic energy demands.

Figure 7 shows the comparison between the 16 vector-valued *IMs* of the second set of *IMs*, those that use in their second component an *IMs* based on the spectral shape, for both models F7 and F10 respectively, the results shown in terms of the standard deviation of the natural logarithm of the maximum inter-story drifts and for a median value of 0.03. As seen in Fig. 7, vector-valued *IMs* that use $Sa(T_1)$, or $Sv(T_1)$, have the best efficiency to predict the seismic response, using N_{pSa}, N_{pSv} or N_{pV} as second component.

Table 6 Optimal T_i and T_f values for the 16 vector-valued spectral shape *IMs* to predict the seismic response of F10 R/C frame

IMs	Inter-story drift		Normalized hysteretic energy	
	T_i/T_1	T_f/T_1	T_i/T_1	T_f/T_1
$<Sa(T_1), N_{pSa}>$	1	2.6	1	2.5
$<Sa(T_1), N_{pSv}>$	1	2.5	1	2.4
$<Sa(T_1), N_{pV}>$	1	2.4	1	2.4
$<Sa(T_1), N_{pEI}>$	1	2.2	1	2.3
$<Sv(T_1), N_{pSa}>$	1	2.6	1	2.5
$<Sv(T_1), N_{pSv}>$	1	2.5	1	2.4
$<Sv(T_1), N_{pV}>$	1	2.4	1	2.4
$<Sv(T_1), N_{pEI}>$	1	2.2	1	2.3
$<V(T_1), N_{pSa}>$	1	2.6	1	2.6
$<V(T_1), N_{pSv}>$	1	2.6	1	2.5
$<V(T_1), N_{pV}>$	1	2.6	1	2.6
$<V(T_1), N_{pEI}>$	1	2.7	1	2.6
$<E_I(T_1), N_{pSa}>$	1	2.7	1	2.5
$<E_I(T_1), N_{pSv}>$	1	2.7	1	2.5
$<E_I(T_1), N_{pV}>$	1	2.7	1	2.5
$<E_I(T_1), N_{pEI}>$	0.1	1.2	1	2.7

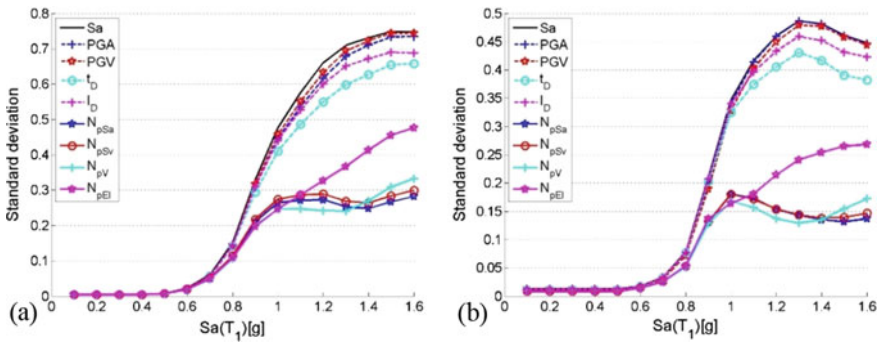

Fig. 3 Efficiency comparison of the standard deviation of the natural logarithm for the maximum inter-story drift of vector-valued *IMs* that use $Sa(T_1)$ as first component for: **a** F7 frame, and **b** F10 frame

4 Conclusions

Several vector-valued ground motion intensity measures have been analyzed with the aim to obtain the best predictor of the structural response in terms of the maximum

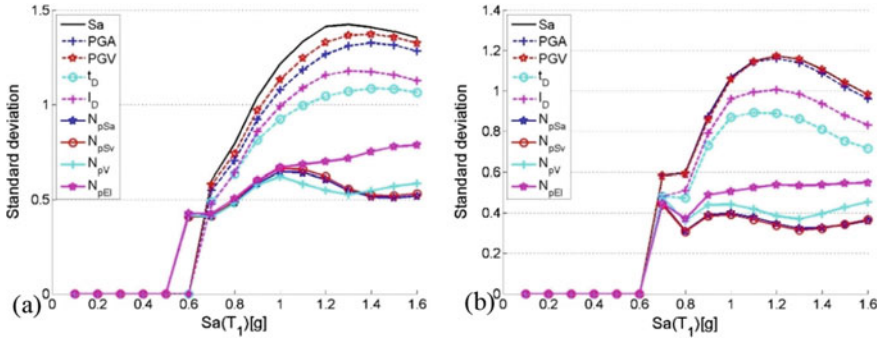

Fig. 4 Efficiency comparison of the standard deviation of the hysteretic energy demands of vector-valued *IMs* that use $Sa(T_1)$ as first component for: **a** F7 frame, and **b** F10 frame

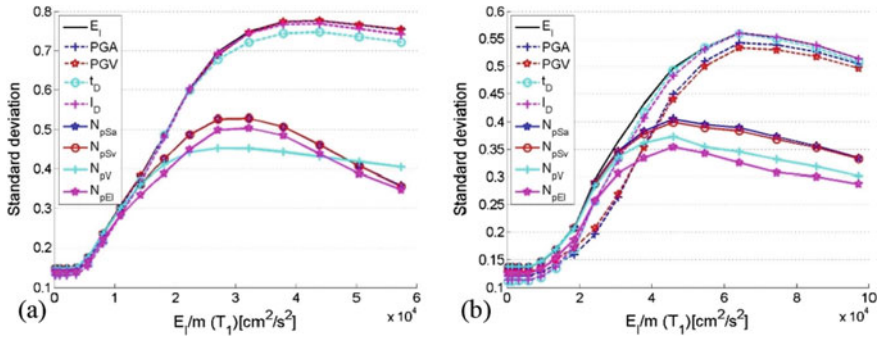

Fig. 5 Efficiency comparison of the standard deviation of the natural logarithm for the maximum inter-story drift of vector-valued *IMs* that use $E_I(T_1)$ as first component for: **a** F7 frame, and **b** F10 frame

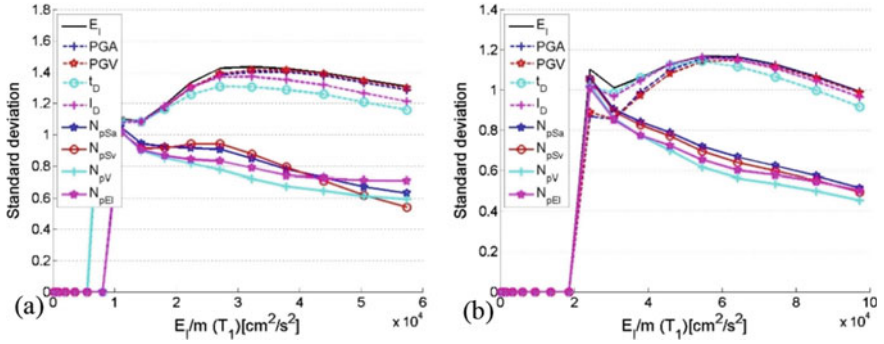

Fig. 6 Efficiency comparison of the standard deviation of the hysteretic energy demands of vector-valued *IMs* that use $E_I(T_1)$ as first component for: **a** F7 frame, and **b** F10 frame

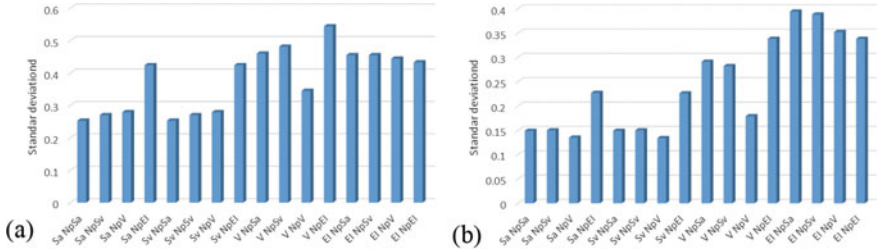

Fig. 7 Efficiency comparison of the standard deviation of the maximum inter-story drifts of vector-valued *IMs* that use *IMs* based on spectral shape as second component for: **a** F7 frame, and **b** F10 frame

inter-story drift and the hysteretic energy demands of 3D R/C frames under narrow-band ground motions. The study considered *IMs* based on peak, cumulative and spectral shape proxies. The numerical study concludes that there is no evidence to support the use of vector-valued *IMs* based exclusively in peak ground motion characteristics for predicting seismic demands of 3D R/C buildings. The results obtained by the vector-valued *IMs* that use $Sa(T_1)$ and $Sv(T_1)$ as the first component of the vector are similar since, they are related, and their efficiency is superior than those obtained using $V(T_1)$ and $E_I(T_1)$ as the first component. The optimization study shows that T_i values equal to T_1, and T_f ranging from 2.0 to 3.0 times T_1, produce an improvement in the prediction of the seismic response. The vectors $<Sa(T_1), N_{psa}>$, $<Sa(T_1), N_{pSv}>$ and $<Sa(T_1), N_{pV}>$ are those that produce the least uncertainty when predicting seismic demands, in such a way that they are very promising to the next generation of advanced vector-valued ground motion intensity measures.

Acknowledgements The authors express their gratitude to the *Consejo Nacional de Ciencia y Tecnología* (CONACYT) in Mexico for funding the research reported in this paper under grant Ciencia Básica 287103 and for the scholarship given to the Ph.D. student. The financial support given by the Universidad Autónoma de Sinaloa under grant PROFAPI is appreciated.

References

1. Housner, G.W.: Limit design of structures to resist earthquakes. In: First World Conference on Earthquake Engineering, Berkeley, California (1956)
2. Arias, A.: A measure of earthquake intensity. In: Seismic Design for Nuclear Power Plants, pp. 438–483. MIT Press, Cambridge, MA (1970)
3. Von-Thun, J.L., Rochin, L.H., Scott, G.A., Wilson, J.A.: Earthquake ground motions for design and analysis of dams. In: Earthquake Engineering and Soil Dynamics II—Recent Advance in Ground-Motion Evaluation, Geotechnical Special Publication 20 ASCE, pp. 463–481 New York (1998)
4. Cosenza, E., Manfredi, G.: A seismic design method including damage effect. In: 11th European Conference on Earthquake Engineering, Paris, France (1998)

5. Mehanny, S.S.: A broad-range power-law form scalar-based seismic intensity measure. Eng. Struct. **31**(7), 1354–1368 (2009)
6. Jamshidiha, H.R., Yakhchalian, M., Mohebi, B.: Advanced scalar intensity measures for collapse capacity prediction of steel moment resisting frames with fluid viscous dampers. Soil Dyn. Earthq. Eng. **109**, 102–118 (2018)
7. Javadi, E., Yakhchalian, M.: Selection of optimal intensity measure for seismic assessment of steel buckling restrained braced frames under near-fault ground motions. J. Rehab. Civ. Eng. **7**(3), 162–181 (2019)
8. Luco, N., Cornell, C.A.: Structure-specific scalar intensity measures for near-source and ordinary earthquake ground motions. Earthq. Spectra **23**(2), 357–392 (2007)
9. Tothong, P., Cornell, C.A.: Structural performance assessment under near-source pulselike ground motions using advanced ground motion intensity measures. Earthq. Eng. Struct. Dyn. **37**(7), 1013–1037 (2008)
10. Baker, J.W., Cornell, C.A.: Vector-valued intensity measures for pulse-like near-fault ground motions. Eng. Struct. **30**(4), 1048–1057 (2008)
11. Yakhchalian, M., Nicknam, A., Amiri, G.G.: Optimal vector-valued intensity measure for seismic collapse assessment of structures. Earthq. Eng. Eng. Vib. **14**(1), 37–54 (2015)
12. Eads, L., Miranda, E., Lignos, D.G.: Average spectral acceleration as an intensity measure for collapse risk assessment. Earthq. Eng. Struct. Dyn. **44**(12), 2057–2073 (2015)
13. Cordova, P.P., Dierlein, G.G., Mehanny, S.S.F., Cornell, C.A.: Development of a two parameter seismic intensity measure and probabilistic assessment procedure. In: The Second U.S.-Japan Workshop on Performance-Based Earthquake Engineering Methodology for Reinforce Concrete Building Structures, Sapporo, Hokkaido, pp. 187–206 (2001)
14. Baker, J.W., Cornell, C.A.: A vector-valued ground motion intensity measure consisting of spectral acceleration and epsilon. Earthq. Eng. Struct. Dyn. **34**, 1193–1217 (2005)
15. Tothong, P., Luco, N.: Probabilistic seismic demand analysis using advanced ground motion intensity measures. Earthq. Eng. Struct. Dyn. **36**, 1837–1860 (2007)
16. Yakut, A., Yilmaz, H.: Correlation of deformation demands with ground motion intensity. J. Struct. Eng. ASCE **134**(12), 1818–1828 (2008)
17. Mehanny, S.S.F.: A broad-range power-law form scalar-based seismic intensity measure. Eng. Struct. **31**, 1354–1368 (2009)
18. Bojórquez, E., Iervolino, I.: Spectral shape proxies and nonlinear structural response. Soil Dyn. Earthq. Eng. **31**(7), 996–1008 (2011)
19. Baker, J.W., Cornell, C.A.: Vector-valued intensity measures incorporating spectral shape for prediction of structural response. J. Earthq. Eng. **12**(4), 534–554 (2008)
20. Buratti, N.: Confronto tra le performance di diverse misure di intensità dello scuotimento sismico. Congreso Nacional de Ingeniería Sísmica Italiano, ANDIS Bari (2011)
21. Buratti, N.: A comparison of the performance of various ground-motion intensity measures. In: The 15th World Conference on Earthquake Engineering (2012)
22. Terán-Gilmore, A.: Consideraciones del uso de la energía plástica en el diseño sísmico. Revista de ingeniería Sísmica SMIS **65**, 81–110 (2001)
23. Bojórquez, E., Ruiz, S.E.: Strength reduction factors for the valley of Mexico taking into account low cycle fatigue effects. In: 13º World Conference on Earthquake Engineering, Vancouver, Canada (2004)
24. Arroyo, D., Ordaz, M.: Hysteretic energy demands for SDOF systems subjected to narrow band earthquake ground motions. Applications to the lake bed zone of Mexico City. J. Earthq. Eng. **11**, 147–165 (2007)
25. Terán-Gilmore, A., Jirsa, J.O.: Energy demands for seismic design against low-cycle fatigue. Earthq. Eng. Struct. Dyn. **36**, 383–404 (2007)
26. Terán-Gilmore, A., Sánchez-Badillo, A., Espinosa Johnson, M.: Performance-based seismic design of reinforced concrete ductile buildings subjected to large energy demands. Earthq. Struct. **1**(1), 69–91 (2010)
27. Bojórquez, E., Ruiz, S.E., Terán-Gilmore, A.: Reliability-based evaluation of steel structures using energy concepts. Eng. Struct. **30**(6), 1745–1759 (2008)

28. Bojórquez, E., Terán-Gilmore, A., Ruiz, S.E., Reyes-Salazar, A.: Evaluation of structural reliability of steel frames: Inter-story drifts versus plastic hysteretic energy. Earthq. Spectra **27**(3), 661–682 (2011)
29. Uang, C.M., Bertero, V.V.: Evaluation of seismic energy in structures. Earthq. Eng. Struct. Dyn. **19**, 77–90 (1990)
30. Trifunac, M.D., Brady, A.G.: A study of the duration of strong earthquake ground motion. Bull. Seismol. Soc. Am. **65**(3), 581–626 (1975)
31. Eads, L., Miranda, E., Lignos, D.: Spectral shape metrics and structural collapse potential. Earthq. Eng. Struct. Dyn. **45**(10), 1643–1659 (2016)
32. Iervolino, I., Manfredi, G., Cosenza, E.: Ground motion duration effects on nonlinear seismic response. Earthq. Eng. Struct. Dyn. **35**, 21–38 (2006)
33. Terán-Gilmore, A., Jirsa, J.O.: A damage model for practical seismic design that accounts for low cycle fatigue. Earthq. Spectra **21**(3), 803–832 (2005)
34. Rodríguez, M.E., Padilla, C.: A damage index for the seismic analysis of reinforced concrete members. J. Earthq. Eng. **13**(3), 364–383 (2008)
35. Bojórquez, E., Reyes-Salazar, A., Terán-Gilmore, A., Ruiz, S.E.: Energy-based damage index for steel structures. J. Steel Compos. Struct. **10**(4), 343–360 (2010)